JKAU: Mar. Sci., **Vol. 31** No. 1 pp: 37-54 (1442 A.H. / 2021 A.D.)
DOI :10.4197/Mar.31-1.4

Microbially Induced Sedimentary Structures (MISS) and their Involvement in Sediment Stabilization and Formation of Gravelly Coastal Landforms (Berms, Spits and Bars) in Salman Hypersaline Lagoon, Red Sea Coast of Saudi Arabia

Ammar A. Mannaa

Department of Marine Geology, Faculty of Marine Sciences, King Abdulaziz University, Jeddah, Saudi Arabia

amannaa@kau.edu.sa

Abstract. This study documents the occurrence of several MISS such as laminated microbial mats, biostabilized ripples, gas domes, mat folds, erosional pockets and remnants, microbial cracks, and gypsified mat chips in Salman hypersaline lagoon, north Jeddah city, Saudi Arabia. This study indicates that both microbial and physical processes are reponsible for sediments biostablization and formation of spits, bars and berms. It focuses on the role of waves generated by winds in erosion of the microbially, biostabilized sediments and their deposition on the eastern shore of the semi-closed Salman lagoon. In winter months, the floor of the lagoon shows a rippled surface that mantled with green to black microbial mats. In summer months, gypsum crystals grow on the surface of the mats and develop a gypsified microbial crust. A slight agitation of the lagoonal water in winter months partially erodes the mat layer and impart a black stain to the water column of the lagoon. In summer months, strong agitation of the waves generated by winds in the lagoon leads to erosion of the gypsified micribial crusts and underlying bioclastic and gypsum layers into gravelly mat chips that leave erosion pockets surrounded with erosion remnants. The gravely, eroded sediments are transported by a longshore current and deposited on the eastern shore of the lagoon as berms, spits and bars. The spits and bars enclose small, shallow pools filled with mud sediments. The result of this study provides useful data to elucidate processes of change in coastal landforms due to bio-stabilization by microbial mats and their erosion by waves induced by wind.

Keywords: Microbial mats, Berms, Spits, Bars, Salman lagoon, Red Sea, Saudi Arabia.

1. Introduction

Studies on microbial mat structures are well known from carbonate (Chafetz and Buczynski, 1992; Andres and Reid, 2006), clastic (Schieber, 1999; Cuadrado *et al*., 2014) and evaporitic (Aref and Taj, 2018; Aref *et al*., 2020) environments. Microbial mats constituted by photosynthetic organisms dominated mainly by cyanobacterial species are commonly colonize shallow and intertidal marine to supratidal sediments (Noffke, 2010; Pan *et al*., 2019; Cuadrado, 2020). The cyanobacteria produce extracellular polymeric substances (EPS) that grow originally on the water-sediment interface as thin biofilms or a thick laminated layer forming a cohesive and leathery carpet that trap, bind and stabilize sediments (Gerdes *et al*., 2000; Stolz, 2000; Noffke, 2010; Stal, 2012; Pan *et al.,* 2019). The EPS has a high water retention capacity that protects the mats from sever desiccation (Or *et al*., 2007; Decho, 2011). The combination of bacteria, EPS and trapped sediments that form microbial mats creates a poorly permeable sediment surface, slowing water percolating from the surface over

periods of time (Bąbel, 2007). In fact, the interaction of microbial mats with physical dynamics have received the particular name of MISS (microbially induce sedimentary structures, *sensu* Noffke *et al*., 2001). The microbial mats flourish in the absence of physical and biological perturbations (Oren, 2010) and develop peaks, ridges, and troughs (e.g., Shepard and Sumner, 2010; Hawes *et al*., 2013; Sumner *et al*., 2016). In the study area of the Salman hypersaline lagoon, the MISS are represented by laminated microbial mats, biostabilized ripples, gas domes, mat folds, erosional pockets and remnants, microbial cracks, and gypsified mat chips.

The term 'bio-stabilization' (*sensu* Paterson, 1994) reports increasing in the critical erosion threshold for the resuspension of particles by bacterial activities that protect the seafloor deposits against erosional processes and increasing the preservation potential of sedimentation (Gehling, 1999; Cuadrado, 2020). Bio-stabilization also includes the sealing of the sediment surface by EPS secreted by micro-organisms (Noffke *et al.,* 2001). Filamentous cyanobacteria in microbial mats provide mechanical strength derived from the linkage of trichomes with the sediment grains and contribute to sediment bio-stabilization by an upward migration during emersion by the excretion of EPS strands (Staats *et al*., 2000; Garwood *et al*., 2015; Cuadrado, 2020). Bio-stabilization by microbial mats altering sedimentary processes and their physicochemical properties in coastal environments (Cuadrado *et al*., 2015), and acts as a biogeomorphological force in sediments (Stal, 2010). The bio-stabilization of sediments alters and increasing the erosive critical threshold in aquatic environments under unidirectional currents (Hagadorn and McDowell, 2012); tidal currents (Noffke, 2010), or even wave-shear stress (Cuadrado *et al*., 2014).

Most of the coastal landforms such as beach ridges and coastal sand dunes form from sea level changes and/or changes of sediment supply affected by climatic change (Koiwa *et al*., 2018), or seismic events in tectonically active areas (Catalán *et al*., 2014; Goff and Sugawara, 2014). However, this study points to the role of microbial mats in bio-stabilization of the sediments that develop into gravely berms, spits and bars by waves induced by winds. Examples from barrier spits composed of gravely sediments are known from recent coastal, marine environments (Stéphan *et al*., 2015; Koiwa *et al*., 2018; Ions *et al*., 2021).

This study shows an example of the formation of gravely berms, spits and bars from the semi-closed, hypersaline Salman lagoon , Red Sea coast of Saudi Arabia that colonized by microbial mats due to its high salinity. In this low energy environment, bio-stabilization by EPS plays a key role in binding fine grained, bioclastic sediment particles and shells of cerithid gastropods. Such microbially-colonized sediments tend to be more resistant to erosional events than mostly abiotic sediments at the floor of the lagoon. The study focus on: (1) the description and interpretation of several MISS with respect to sediment composition, hydrodynamics and geomorphology, and (2) the description and interpretation of the formation of the coastal landforms in the eastern part of the lagoon such as berms, spits, bars and intervening pools.

2. Study Area

The Red Sea coast of Saudi Arabia consists mainly of Pleistocene and Recent reef complexes that occasionally disconnected with hypersaline lagoons. The lagoons are dominantly surrounded with supratidal-intertidal sabkhas. There are over twenty lagoons (sharms, khors or khawrs) along the

1832 km stretch of the Red Sea coast of Saudi Arabia (Rasul, 2015). The studied hypersaline Salman lagoon is located east of Dhahban area, 50 km north of Jeddah city (Fig. 1). The lagoon has different synonymies as appeared in the literatures, such as Hatiba lagoon (Meshal, 1987), Ras Hatiba lagoon (El-Sayed, 1987), Sulaymaniya lagoon (Bahafzullah *et al*., 1993), Salman Bay (Youssef, 2015; Hariri and Abu-Zied, 2018), Khalig Salman (Youssef, 2015), or Salman lagoon (Aref *et al*., 2020). The lagoon is an isolated and elongated water body that extends parallel to the Red Sea coast for about 13km with NNW-SSE direction. It is connected to Red Sea by a narrow (about 70-160 m wide) and shallow (20-50 cm in depth) tidal channel. The lagoon water is hypersaline (salinity ranges from 51-113‰), with a water depth < 2.5 m deep and it has an elliptical surface area of 30 km^2. The bottom sediments of the lagoon consist of dominant bioclastic, and few siliciclastic coarse sands with small patches of fine silt and clay sediments. The lagoon is bounded at north, south and west by a raised beach and Pleistocene coral limestone (1.5 to 2 m high), and at east and southeast by sabkha having gypsum and halite mixed with sand (El-Sayed, 1987). The eastern coast of the lagoon contains berms, bars, spits and intervening shallow pools.

Two hypotheses explain the formation of the Red Sea lagoons. The first hypothesis advocates that the lagoons were former channels formed by erosion in the Late Pleistocene that were drowned by the post-glacial rise in sea level (Brown *et al*. 1989). Wadies directly drained these lagoons during the last glacial period when the sea level was lowered by at least 140 m. The second hypothesis assumed that the lagoons are remnants of collapse features formed during post-warming (postglacial?) emergence by selective dissolution of Miocene evaporite beds underlying the younger succession (Rabaa, 1980).

The size and shape of lagoons and associated channels are dependent on the current velocity, wave energy and tidal range. Al-Barakati and Ahmad (2012) pointed out that currents are usually weak inside the lagoons and are governed by both the spring–neap tidal cycles and fluctuation in the water level. Wind stress also plays a dominant but variable role in the process of sediment transport, depending on the strength of the local tides and wind speed (Ahmad and Sultan, 1992), whereas the strength of the wave energy controls the shape of the lagoons (Rasul, 2015). The lagoon margins are bounded by intertidal flats and sabkhas that extend to a few kilometers inland from the shoreline (Aref *et al*., 2020). Rasul (2015) considered tides as of primary importance because they provide a periodic exchange of water through channels connecting the lagoons to the sea.

3. Climate and Hydrography

The study area is characterized by scarce annual rainfall of 6 cm in the winter months, and high annual evaporation of 205 cm. Mean daily temperatures range from a minimum of 26.7ºC in January to a maximum of 39.3ºC in July. The humidity ranges from 19% in winter time to 100% in summer time. The winds blow from north and northeast in summer, and north and northwest in winter with a speed range from 4 to 10 km/h (PME, 2015). The pH value of the lagoonal water ranges from 8.03 (in October) to 8.14 (in February), and the average water temperature is about 33.4ºC which is relatively higher than the Red Sea water value 28.6º (Meshal, 1987). The water salinity of the lagoon increases from 55‰ (at north) to 70-110 ‰ (at south), whereas the salinity of Red Sea is approximately 40‰ (Aref *et al*., 2020). The tidal range in the

lagoon is small (8 cm) because the lagoon is close to the nodal zone. This tidal force is dominating the water circulation in the lagoon (Ahmed *et al*., 1989; Al-Barakati, 2011).

4. Methods of Study

This study is based on field examination of the lagoon in October 2008, 2012, December 2016 and January 2021. During the field work, the coastal landforms of the lagoon are photographed, measured and sampled. The sediment samples are collected from the shallow bottom and shore of the lagoon. In addition, two cores were drilled at the eastern margin of the lagoon by introducing manually 130 cm long PVC tubes. The salinity and density of the lagoonal water are measured in the field with glass hydrometers, and the brine temperature is measured with a glass thermometer.

5. Results

5. 1 Microbially Induced Sedimentary Structures (MISS)

Several MISS were found in the intertidal and shallow subtidal parts of Salman lagoon such as microbial domes, microbial folds, biostabilized ripples, erosion pockets and remnants, microbial cracks, and microbial chips. The floor of the lagoon is covered with yellowish green microbial mats over black decayed mats. In the subsurface, the sedimentary sequence consists of laminated, dark microbial layers and white bioclastic layers that may show gas escape structure.

5. 1. 1 Laminated microbial mats

Laminated microbial mats occur in the lagoon at water depths less than 40 cm. Microbial mats exist as varicolored, green, yellow, mauve or red, cohesive, leathery, gelatinous, thick (>2 cm) cyanobacteria (Fig. 2a). At salinity less than 70‰, benthic gastropods (*cerithium* sp.) flourish on the floor of the lagoon and graze over microbial mats. Burial of the mats due to increased supply of suspended bioclastic sediments lead to the death and decay of the mats. The result is laminated sediments composed of black, organic matter-rich laminae and bioclasts-rich laminae (Fig. 2b).

5. 1. 2 Biostabilized ripples

The shallow subtidal part of the lagoon is covered with asymmetrical and symmetrical ripple marks (Fig. 2c and d). The height of the crests is less than 5 cm and the wave length ranges from 15 to 20 cm. A thin, leathery, gelatinous, yellow diatom biofilm colonizes the uppermost sediments that underlain with a thin, green, epibenthic microbial mat layer, dominated with filamentous cyanobacteria (Fig. 2d), similar to the observations of Pan *et al*. (2019). The diatom and cyanobacteria colonize and stabilize the sediment surface of ripples. The mat layer is thicker in depressions (1.5 mm) and thinner (0.3 mm) on top of ripples, similar to the observations of Cuadrado (2020). Below the green cyanobacterial mat, there is a purple layer rich in sulfur bacteria. The subsurface sediments below the surface mat layers show anoxic condition due to the dominance of sulfate-reducing bacteria (Figs. 2a and b), (Pan *et al*., 2019).

5. 1. 3 Gas domes

This structure usually takes a circular to slightly elliptical shape in a horizontal plane view, and domal shape in a vertical plane view (Fig. 2e). The domes range in diameter from 2 to 5 cm, with a height less than 3 cm. The upper surface of domes consists of 2-4 mm thick, green cyanobacterial mat layer over dark grey to black laminated, microbial mat and bioclastic layers. The upper surface of domes are generally smooth or may show a hollow at the crest of domes (Fig. 2e). Below the cyanobacterial layer is a hollow filled with organic gases from decay of the subsurface microbial mats. In summer months, the domes

are encrusted with 5-7 cm thick gypsum layer to form gypsified gas domes (Fig. 3a). The gypsum domes enclose a hollow filled with organic gases. The subsurface sediments below gypsum domes show injected, vertical to slightly inclined veins and domes of white bioclastic materials within the black microbial layers (Fig. 3b).

5. 1. 4 Mat folds

This structure usually takes an elongated, slightly twisted microbial folds in a horizontal plane view (Fig. 3c). In a vertical profile, the folds show a vertical convex-upward layer with intervening concave-downward depressions (Fig. 3d). Several folds show different orientations that may intersect with each other. The upper surface of folds consists of 3-6 mm thick, green cyanobacterial layer. The underlying sediments are laminated that commonly show a wavy structure compromise to the surface microbial fold (Fig. 3d).

5. 1. 5 Erosional remnants and pockets

Erosional remnants and pockets are composed of an elevated, flat-topped surface portions, and intervening depressions floored with ripple marks, respectively (Fig. 4a, b). Erosional remnants are overgrown by green, brown to black microbial mats. The erosional remnants range in height from 5 to 8 cm, extend laterally from 5 to 20 cm, and show a high slope angle at their prepheries. In a vertical cross-section, the remnants are overgrown with green microbial layer that underlains with dark grey to black lamination of buried microbial mat laminae, alternating with white bioclastic layers. The erosional pockets exist between the remnants and are commonly not overgrown by microbial mats. The floor of pockets are covered with ripple marks that show the same orientation to that of the surrounding mat-free sediment surface of the lagoon. The ripple marks indicate the direction of the waves induced by winds that form the erosional pockets. The erosional pockets may exist as light, yellow patches within the dark, black color of the surrounding remnants (Fig. 4c). The eroded microbial filaments from the erosion pockets are floating in the water column of the lagoon and is responsible for its black coloration (Fig. 4d).

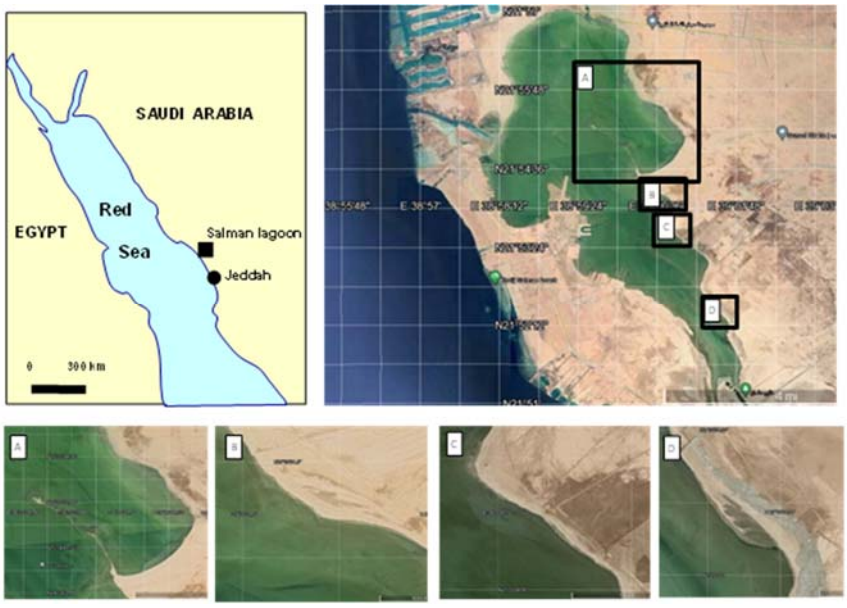

Fig. 1. Location map of the study area, and satellite images showing the location of spits and bars in Salman lagoon.

Fig. 2. Laminated microbial mats, ripples and gas domes. (a) Leathery, gelatinous, varicolored microbial mats overlying organic matter-rich sediments. (b) laminated, dark microbial mats and light bioclastic layers. (c) Ripple marks close to a spit and biostabilized by microbial mats. (d) Biostabilized ripples that contain coarse bioclasts and gastropod shells. (e) Gas domes in the surface mat layer.

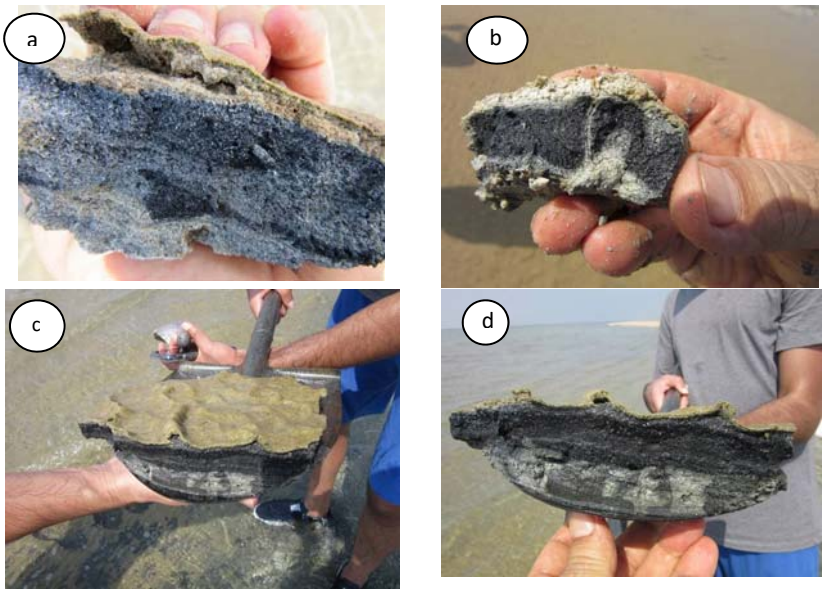

Fig. 3. Gypsified gas domes and microbial folds. (a) A hollow beneath gypsified gas domes overlying organic matter-rich bioclastic sediments. (b) A white, fluidized sediments inject the organic matter-rich zone to form gas domes. (c) Irregular, polygonal folds on the surface of microbial mats. (d) A convex-upward crests, and concave downward troughs in polygonal folds that overlie wavy, organic matter-rich laminae.

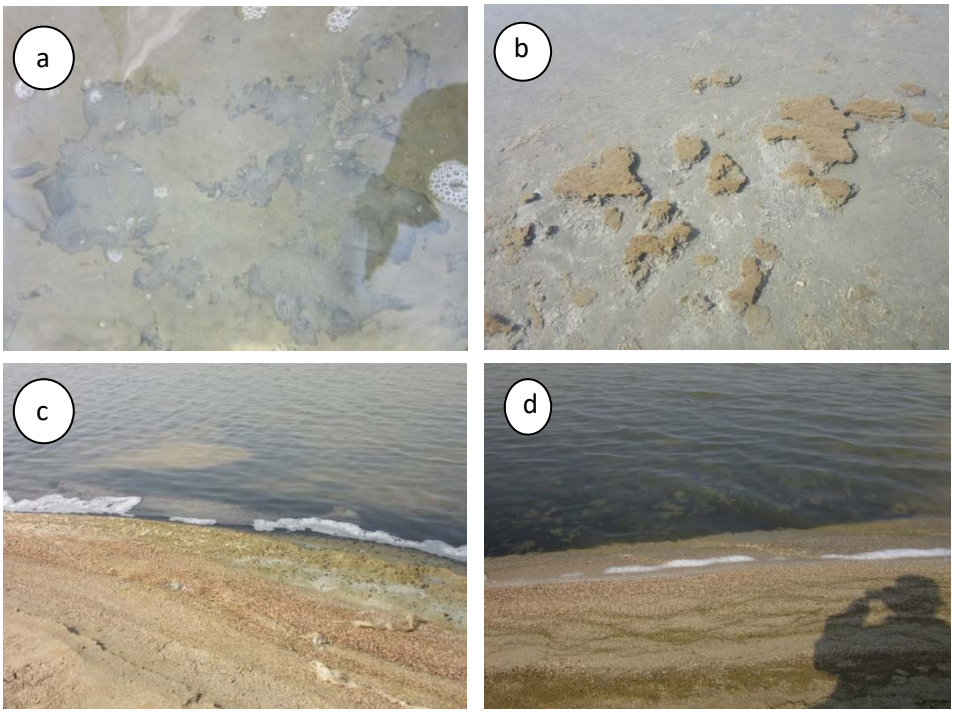

Fig. 4. Erosion pockets and remnants. (a) A subaqueous, erosion pockets surrounded with erosion remnants. (b) Erosion remnants show high elevation that surrounded with erosion pockets. (c) A light-colored zone of erosion pockets surrounded with black zone of erosion remnants highly enriched in black, microbial layers. (d) Black color of the water of lagoon due to suspended organic matter from the erosion pockets.

5. 1. 6 Gypsified mat chips

Microbial mat chips are recorded as detached fragments of flattened or slightly curved microbial mat at the shallow part of the lagoon (Fig. 5a). They are recorded on the down current direction of erosion remnants and pockets. They are spread over recently developed microbial mat layer. They are also dominating the coastal bars, spits and berms. The wet mat chips have a green or yellowish green color (Fig. 5b). Also, the dry mat chips show white or beige color (Fig. 5c). The mat chips range in thickness from 3 to 6 mm, and diameter ranges from 2 to 4 cm. They are composed of gypsum crystals and bioclastic grains that are firmly attached with green cyanobacterial filaments (Fig. 5b). The gypsified mat chips are derived from gypsified microbial layer or gypsified gas domes that are easily separated from the underlying bioclastic sediment layer. The mat chips expose high cohesiveness and plasticity that resist further disintegration into small pieces in the sand size. The mat chips have rounded edges that differ in geometries from mud clasts, similar to observation by Noffke (2010).

5. 1. 7 Microbial cracks

In the study area, lowering of the water level of the lagoon due to summer fall in seawater and/or evaporation leaves microbial mats subjected to desiccation and cracking. In a plane view, microbial cracks form polygons with smooth outlines (Fig. 5d). In a vertical profile, the cracks occur only in the surficial zone of the black microbial mats and have a wedge-shape that pointing downwards. The substrate bioclastic sediments immediately below the microbial cracks show irregular layering and not affected by cracking. Most cracks are partially filled with bioclastic

sediments that derived during tidal storms (Fig. 5d).

5. 2. Subsurface Sediments

Two cores in the eastern shore of the lagoon exhibit a few millimeters to several centimeters thick alternation of gravel, sand and mud laminae or layers (Fig. 6). The subsurface sedimentary section consists of a laminated structure from black, mud-rich microbial laminae that may be encrusted with gypsum layer and a benthic, cerithid-rich, bioclastic layers. The contact between laminae and layers is sharp, planar or wavy, with occasional occurrence of deformed horizons. The gravel layers are 5-10 cm thick and composed of aggregates of cerithid gastropod shells. The sand laminae (or layers) are composed of bioclasts or gypsum crystals and may include sponge pore fabrics. These pores are regarded as a secondary high porosity typical for sand intercalated between two buried mat layers caused by gases derived from bacterial metabolic activity (Noffke, 2010; Cuadrado, 2020). The thin, deep black, organic matter-rich laminae in the cores represent decayed, buried microbial mats (Noffke, 2000; Noffke *et al*., 2002 and Cuadrado, 2020). The lamination of the subsurface sediments indicates the fluctuation in the salinity that controls the type of flourishing organisms, whereas the seasonal variation in sea level and hydrodynamic control the persistence or erosion of the sediment materials (Cuadrado, 2020).

5. 3. Berms, Spits and Bars

Berms (or beach ridges according to Otvos, 2020) are recorded as 3 successive ridges at the coast, where they mark the successive high tide levels that follow the spring tide through to the neap tide. Berms show narrow, wedge-shaped shore ridges, located on the upper foreshore. The berm ridges form shore-parallel linear bodies of triangular cross section (Fig. 7a). Their seaward slope is steeper than the landward-inclined side. They are composed of gravel sized particles of gypsified mat chips, bioclasts and gastropod shells (Fig. 7b). Similar berms composed of cobble-to-boulder-sized clastics are recorded by Sander *et al*. (2019), and Ions *et al*. (2021).

Several spits and bars occur at the eastern coast of hypersaline Salman lagoon (Fig. 1). Spits occur as extended stretch of beach materials that project out to the lagoon and they are attached at their proximal end to the mainland (Fig. 7a, b), whereas bars are joined with the mainland from both directions. The length of spits and bars, and their submerged shoal range from 130 to 1700 m, and width from 70 cm to 10 m. The distal part of spits may be varied according to the local hydrodynamic conditions and the amount of sediment materials (Fig. 7c), similar to observation by Krylenkoa *et al*. (2018). Spits and bars may curve inwards at the seaward side and at the distal part due to wave refraction (Fig. 7c, d). The spits and bars are composed of gravel sized bioclastic materials, gypsum clasts and gastropod shells (Fig. 7e). The spits and bars are separated from the coast with small pools that floored with finer sediments (Fig. 7f). The pools have a calmer water that sheltered by the spits and bars. They also enclose several runnels that extend normal to the coastline and filled with grey, muddy sediments (Fig. 7f).

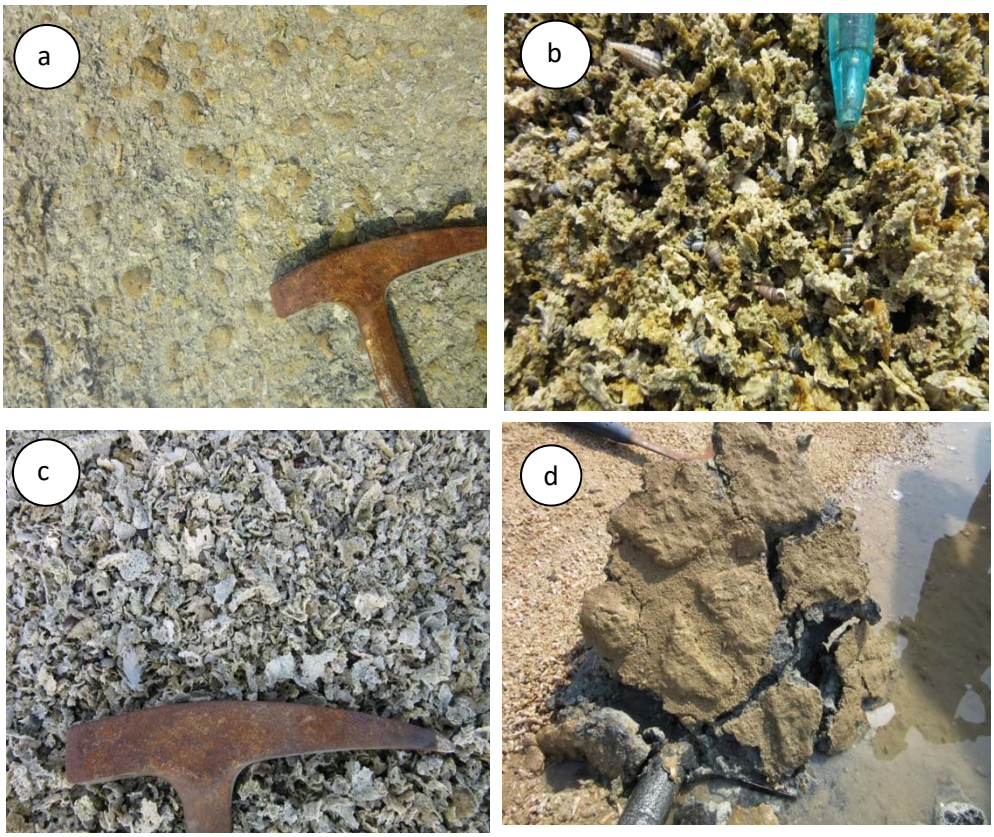

Fig. 5. Mat chips and microbial cracks. (a) Gypsified mat chips scattered on the floor of the lagoon. (b) Mat chips and gastropod shells with greenish yellow color from microbial filaments. (c) Gypsified mat chips, bioclasts and gastropod shells thrown to the margin of the lagoon. (d) Polygonal, microbial cracks filled with bioclastic sediments.

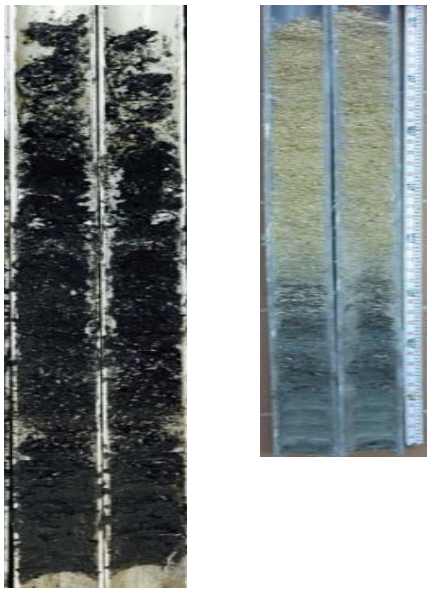

Fig. 6. Two cores from the eastern coast of the lagoon. The black core is from the intertidal zone and it is highly enriched in organic matter. The light core is from the coastal berms and shows an upper mat chips, bioclasts and gastropod shells, and a lower black, organic matter rich sediments.

Fig. 7. Berms, spits and bars. (a) A coastal berm and spits separated with a shallow pool. (b) A trench in the berm shows several layers from gravel-sized, mat chips, bioclasts and gastropod shells. (c) A spit join to the mainland at one end and projecting to the lagoon at the distal end. (d) A zigzag boundary of the spits due to wave action induced by winds. (e) Cross-section in a spit showing a seaward cliff and a landward gently sloping side. The sediments are generally

gavel-sized, mat chips, bioclasts and gastropod shells. (f) A pool between spit and berm shows runnels normal to the coast and consist of grey mud sediment.

6. Discussion

6. 1 Formation of MISS

6. 1. 1 Laminated microbial mats and sediment biostabilization

The occurrence of microbial mats in the lagoon indicates the high productivity of cyanobacteria due to the absence of grazers or predators, a low salinity value below gypsum saturation level, and good light penetration in very shallow waters, similar to interpretation by Cornée *et al*. (1992), and Aref *et al*. (2021). The mats form tight and impervious layers that form a barrier between underlying sediments and brines. This impedes gas and solute transfer and enhances reducing conditions in the underling black sediments (Fig. 2a). The laminated structure of microbial mats with gypsum and bioclastic sediments (Fig. 2b, 3d) reflects the interplay between biological and physical factors (Jorgensen *et al*. 1983). The biological factor is represented by the flourishing of cyanobacteria under a certain salinity range (70-150‰), absence of grazers, slight wave agitation and shallow depth of the water column. The physical factors that limit growth of microbial mats are high salinity, strong waves and supply of much bioclastic and siliciclastic materials. The bio-stabilization of the bioclastic sediments of the intertidal area of the lagoon is due their trapping and binding by microbial filaments (Gerdes *et al*. 1993). Hagadorn and McDowell (2012) indicated that the bio-stabilization process is due to the entangling of the sedimentary grains by cyanobacterial filaments and the role of extracellular polymeric substances (EPS) to adhere grains into a cohesive matrix. The bio-stabilization protects sedimentary surface overgrown by microbial mats against erosion (Noffke and Paterson, 2008). Bio-stabilization may result into some structures such as gas domes and erosional pockets (Noffke, 2010; Maisano *et al*., 2019).

6. 1. 2. Formation and primary preservation of ripples

In winter months, the relatively high sea level of the Red Sea transport suspended sediments to the lagoon (Al-Barakati, 2011). The increased water depth to 40 cm at the eastern and southern margins of the lagoon, waves and currents generated by northwestern wind have sufficiently high flow velocity to allow transport of sediment particles. Such waves and currents form symmetrical and asymmetrical ripples that may be created over the microbial mats of the last summer season (Fig. 2c, d). In the summer months, the lowering of the sea level and the decreases in the amount of transported and suspended sediments, in addition to the increased salinity of the lagoon favor the development of epibenthic microbial mats atop the ripples due to a rapid motility of the filaments (Shepard and Sumner, 2010), leading to their bio-stabilization. Cuadrado (2020) noted that the rapid reorganization of microbial mat fabrics stabilizes ripple marks when the sedimentation ceases through binding of sedimentary particles and creation of an organic layer covering ripple marks.

The sediment surface of the shallow subtidal and intertidal zones is overgrown by epibenthic microbial mats, which are typical in intertidal and supratidal zones (Noffke, 2010; Cuadrado, 2020). The cyanobacteria secrete large amounts of EPS as a protection against desiccation when the submerged sediments are exposed. Such a slippery mat surface reduces the frictional forces of the water flow and protecting the underlying sediment from erosion by moderate currents, and only strong

currents can damage them (Noffke, 2010; Pan *et al*., 2017).

6. 1. 3 Formation of gas domes

Gas domes were described from modern tidal flats in arid and temperate humid climatic zones, and also in supratidal and subaqueous areas (Noffke, 2010; Bose and Chafetz, 2011; Aref and Taj, 2018). They occur with thick, epibenthic microbial mats that seal tidal deposits (Noffke, 2010). Gas domes result from upward, pressurized, intra-sedimentary organic gases that produce a flexible deformation of biofilm or microbial mat (Noffke, 2010; Maisano *et al*., 2019). The organic gases such as O_2, CO_2 and CH_4 are produced by microbial activity, photosynthesis and decomposition (Gerdes *et al*., 2000; Schieber, 2004). Noffke (2010) mentioned that gas domes are associated with the normal high-water line due to the pushing of gases by the rising tide. In the study area, the injected, white sediments within black, decayed microbial layers (Fig. 3b) may result from fluidization of the subsurface sediments by pressurized organic gases and/or pore water due to tidal or wave effect, similar to observation by Taj *et al*. (2014), and Maisano *et al*. (2019).The fluidization process of the underlying white bioclastic sediments result from the tidal and/or wave action on the water column that produces their temporal fluid behavior. The entering sea water percolates through the sediment, pushing air and gases through sedimentary pores forming gas domes at the surface (Figs. 2e, 3a). Gas domes develop due to microbial gassing (from O_2 production through photosynthesis or CO_2 production due to bacterial activity and organic matter decay), underneath EPS-rich microbial mats constructed by filamentous cyanobacteria, which avoid much of the fluid exchange of gases between underlying and the water or atmosphere above (Fig. 2a) (Noffke, 2010 and Cuadrado *et al*., 2015). Therefore, gas accumulates underneath the sealing flexible mat and its pressure lifts it, losing contact with the underlying substrate and generating a hollow cavity (Fig. 3a). After dry condition, the microbial mat maintains the separation from the underlying sediments.

6. 1. 4 Mat folds

The mat folds are formed through migration of subsurface organic gases from buried microbial mats that entrapped below the impermeable barrier, surficial, leathery microbial mats. Lateral movement of the escaped gases below the slippery surface of the mats produced variable shapes of polygonal folds according to the slope of the sediment surface (Fig. 3c, d). Reineck *et al*. (1990) and Cornée *et al*. (1992) mentioned the role of subsurface gas pressure in the origin of polygonal folds (petee structures). Gerdes *et al*. (1993) interpreted the formation of folds as due to the interplay between bio-stabilization of the sediment surface by microbial mats, decay of subrecent mats and gas production in the subsurface. The effect of tidal current and waves induced by wind is pushing the organic gases in the sediment pores to move to the surface making doming and folding of the surface mat layer (Noffke, 2010) and the separation of the surficial mat from the underlying sediment.

6. 1. 5 Erosional pockets and remnants

Strong waves induced by winds at the shallow margin of the lagoon detached the microbial mats from the floor leaving erosion pockets (Fig. 4a-c). This turns the clear water of the lagoon to slightly turbid, brownish or reddish color due to floating, detached, reddish, microbial filaments (Fig. 4d), similar to observation by Davis (2006). The erosional remnants with higher slope angles indicate microbial mats with higher bio-stabilization properties than remnants having lower slope angles (Noffke, 2010).

6. 1. 6 Microbial cracks

Microbial cracks result from subaerial exposure and desiccation of microbial mats (Noffke, 2010). The intimate occurrence of polygonal shallow cracks in the waterlogged, microbial mats and their absence in the underlying sediments (Fig. 5d) is due to shrinkage of the surface mat layers **(**Kovalchuk *et al*., 2017**).** Shrinkage of the mats through bringing the entangled sediment grains into a closer packed arrangement is highest at the sediment surface and decrease downward to develop V-shaped cracks (Kovalchuk *et al*., 2017**).** The underlying sediments that are free from microbial mats preserve the pore spaces and are not contracted. The fluctuation in the tidal water levels favors bio-stabilization, desiccation and shrinkage of the mats that exceed their tensile strength during low tide, and filling of the microbial cracks with bioclastic sediments during high tide (Fig. 5d), similar to the interpretation of Noffke *et al*. (2001), and Porada *et al*. (2007). Kovalchuk *et al*. (2017) indicated that the cohesive nature and heterogeneous distribution of microbial mats prevents the formation of a regular crack network.

6. 1. 7 Gypsified mat chips

The occurrence of mat chips indicate the high energy events of waves or currents induced by surface winds in the semi-closed nature of the hypersaline Salman lagoon. The strong waves or currents partially erode the microbial mat layer into erosion pockets surrounded with erosion remnants (Fig. 4a-c). The eroded mat fragments are deposited close to the edges of erosional remnants (Fig. 5a), where the underlying bioclastic grains underneath the microbial mat are washed away. The fringes of the undermined mat tear and break off into pieces. These fragments are transported by currents and distributed randomly on the depositional surface (Fig. 5b, c). The rounded edges of mat chips may result from erosion during transport across the sedimentary surface, or from continuous growth of the mat (Noffke, 2010). The accumulation of mats chips in the coastal landforms of bars, spits and berms support the strong cohesion of the mats chips during transportation to the shore.

6. 2 Formation of Berms, Spits and Bars

The sediments of the Salman berms, spits and bars are derived from the nearby, shallow subaqueous gypsified microbial mats. The abraded fragments of erosion pockets (Fig. 4a-c) are drifted to the shore by strong waves induced by wind action. In wintertime, the high sea level of the lagoon coupled with strong waves induced by wind transport the gravely gypsified mat chips, bioclasts and gastropod shells to the coast forming berms at several levels (Fig. 7a, b). The strong swash pushes these gravely sediments up the beach at an angle. The weaker backwash brings fine mud sediments straight out that follows the gradient of the beach (Fig. 7f). In summertime, the low sea level of the lagoon is below the coastal berms. Strong waves induced by winds form a longshore current that transport the coastal sediments in a zigzag pattern further along the beach by longshore drift (Fig. 7d). When the swash is stronger than backwash results in deposition of sediments at the spits. The direction of waves influences the direction of longshore drift.

The prevailing northwest wind pushes the waves at an oblique angle toward the shore, where the waves pick up sediment from erosion pockets and swash it up the beach at an angle. The retreat of waves by weak backwash drags fine sediment particles (Fig. 7f). Such longshore drift of sediments in a zigzag pattern builds up deposited sediments

to form a spit, with a curved end because of the waves pushing sediments inland (Fig. 7d).

The occurrence of spits at some parts of the eastern side of the lagoon and their absence in the northern, southern and western sides (Fig. 1) is related to the direction of the prevailing wind with respect to the coastline. The strong northwest blow of wind towards the eastern coast of the lagoon result into longshore drift of sediment particles and formation of spits.

The continuous supply of sediments to the spits may lead to their further extension and elongation to form a bar, which join the mainland from both directions. The bar becomes a stable landform if it is not breached by the lagoonal water.

7. Conclusion

The main factor controlling the deformation of microbial mats and formation of the coastal landforms is the intensity of waves induced by surface winds. The hypersaline Salman lagoon is a semi-closed system that disconnected from the Red Sea with a Quaternary coral reef barrier that prevent sea waves from reaching of the lagoon. In addition, the small tidal range in the area has a limited effect in the formation of coastal landforms. Moreover, slow currents (0.5 m/s) under weak winds may easily uplift ripped gypsified microbial fragment from the underlying sediment due to the action of the shear stress over the bottom (Noffke, 2010).

In winter time, waves generated by wind and tidal currents in the lagoon create wave and current ripples before flourishing of microbial mats. In the summer months, increasing in the salinity of the lagoonal water favors growth of microbial mats atop of ripples and lead to their bio-stabilization. Gas domes on the surface of microbial mats are formed by escaping of subsurface gases through the sediment from decayed microbial mats. The gases may be derived also from the effect of tidal water on entrapped, subsurface gas-filled sponge pores beneath the microbial mats. However, despite that the lagoon is semi-closed and it is protected from strong waves of the Red Sea by a Quaternary reefal terraces, the high speed of the winter time, northwestern wind initiates storm waves, up to 2 m high. These waves created erosional pockets due to the detachment of the microbial mats from the underlying sediment. In Rabigh lagoon, north of the studied Salman lagoon, Al-Barakati and Ahmed (2012) found that the tidal current velocity varied from about 0.05 m/s to about 0.2 m/s depending on the spring-neap cycle and the seasonal variations of the mean sea level in the Red Sea, whereas the tidal currents at the inlet are faster owing to the narrowness of the entrance. If the speed of tidal current is similar to that in Rabigh lagoon, then the main controlling factor in the formation of the berms, spits and bars is the speed of wind that initiates waves capable to detach and transport the gypsified mat layer into the coast.

References

Ahmad, F., Sultan, S.A.R., and **Moammar, M.O.** (1989). Monthly variations of the net heat flux at the Air-Sea interface in coastal waters near Jeddah, Red Sea". *Atmosphere-Ocean*, **27**(2): 406-413.

Ahmed, F. and **Sultan, S.A.R.** (1992). The effect of meteorological forcing on the flushing time of Shuaiba Lagoon on the eastern coast of the Red Sea. *JKAU. Mar. Sci.,* **3**: 3-9.

Al-Barakati, A.M.A. (2011). A hydrographic study of Ras Hatiba Lagoon, *Red Sea International Journal of Engineering & Technology IJET-IJENS,* **11**(02): 48-64.

Al-Barakati, A.M.A. and **Ahmad, F.** (2012) Water column conditions in a coastal lagoon near Jeddah, Red Sea. *Oceanologia*, **54** (4): 675–685.

Andres, M.S. and **Reid, R.P.** (2006). Growth morphologies of modern marine stromatolites: A case study from Highborne Cay, Bahamas. *Sedimentary Geology*, **185**: 319-328.

Aref, M.A. and **Taj, R.** (2018). Recent evaporite deposition associated with microbial mats, Al Kharrar supratidal–

intertidal sabkha, Rabigh area, Red Sea coastal plain of Saudi Arabia. Facies 64, 28: 1-23.

Aref, M.A., Taj, R. and **Mannaa, A.** (2020) Sedimentological implications of microbial mats, gypsum, and halite in Dhahban solar saltwork, Red Sea coast, Saudi Arabia. *Facies,* **66**:10, 1–18.

Bąbel, M. (2007). Badenian Gypsum Facies as a Model Salina-Type Basin Deposit. In: Schreiber, B.C., Lugli, S., Babel, M. (Eds.), *Evaporites through Space and Time*. Geological Society of London, London, Special Publication, 107–142.

Bahafzullah, A.A.K., Fayed, L.A., Kazi, A. and **Al-Saify, M.** (1993). Classification and distribution of the Red Sea coastal sabkha near Jeddah, Saudi Arabia. *Carbonates and Evaporites,* **8**: 23-38.

Bose, S. and **Chafetz, H.S.** (2011). *Morphology and distribution of MISS: A comparison between modern siliciclastic and carbonate settings. Microbial mats in siliciclastic depositional systems through time*. Special Publication 101. SEPM Society for Sedimentary Geology, Tulsa, pp. 3–14

Brown, G.F., Schmidt D.L. and **Huffman A.C.** (1989). *Shield area of western Saudi Arabia. Geology of the Arabian Peninsula*, U. S. Geol. Survey Prof. Paper. No.506-A.

Catalán, P.A., Cienfuegos, R. and **Villagrán, M.** (2014). Perspectives on the long-term equilibrium of a wave dominated coastal zone affected by tsunamis: the case of Central Chile. *J. Coast. Res*., **71**: 55-61.

Chafetz, H.S. and **Buczynski, C.** (1992). Bacterially induced lithification of microbial mats. *Palaios,* **7**: 277–293.

Cornée A., Dickman, M. and **Busson, G.** (1992). Laminated cyanobacterial mats in sediments of solar salt works; some Sedimentological implications. *Sedimentology,* **39**: 599-612.

Cuadrado, D.G. (2020) *Geobiological model of ripple genesis and preservation in a heterolithic sedimentary sequence for a supratidal area*. Sedimentology, doi: 10.1111/sed.12718.

Cuadrado, D.G., Pan, J., Gómez, E.A. and **Maisano, L.** (2015). Deformed microbial mat structures in a semiarid temperate coastal setting. *Sedimentary Geology*, **325**: 106-118.

Cuadrado, D.G., Perillo, G.M.E. and **Vitale, A.** (2014). Modern microbial mats in siliciclastic tidal flats: evolution, structure and the role of hydrodynamics. *Mar. Geol.,* **352**: 367–380.

Davis, S.C., Martinez, L. and **Kirsner, R.** (2006). The diabetic foot: The importance of biofilms and wound bed preparation. Curr. *Diabetes Rep*., **6**: 439-445.

Decho, A.W. (2011). Extracellular Polymeric Substances (EPS). In: Reitner, J., Thiel, V. (Eds.), Encyclopedia of Geobiology, *Encyclopedia of Earth Sciences Series*. Springer, Netherlands, pp. 359-362.

El-Sayed, M. Kh. (1987). Chemistry of modern sediments in a hypersaline lagoon, north of Jeddah, Red Sea. Estuarine, *Coastal and Shelf Science*, **25**: 467-480.

Garwood, J.C., Hill, P.S., MacIntyre, H.L. and **Law, B.A.** (2015). Grain sizes retained by diatom biofilms during erosion on tidal flats linked to bed sediment texture. *Cont. Shelf Res*., **104**: 37-44.

Gehling, J. (1999) Microbial mats in terminal Proterozoic siliciclastics: Ediacaran death masks. *Palaios*, **14**: 40–57.

Gerdes, G., Claes, M., Dunajtschik-Piewak, K., Riege, H., Krumbein W.E. and **Reineck H.E.** (1993) Contribution of microbial mats to sedimentary surface structures. *Facies*, **29**: 61-74.

Gerdes, G., Krumbein, W.E. and **Noffke, N.** (2000). Evaporite microbial sediments. In: R.E. Riding and S.M. Awramik (Eds), *Microbial Sediments*, pp. 196-208. Springer; Berlin.

Goff, J. and **Sugawara, D.** (2014). Seismic-driving of sand beach ridge formation in northern Honshu, Japan? *Mar. Geol.,* **358**: 138-149.

Hagadorn, J.W. and **McDowell, C.** (2012). Microbial influence on erosion, grain transport and bedform genesis in sandy substrates under unidirectional flow. *Sedimentology,* **59**: 795-808.

Hariri, M.S.B. and **Abu-Zied, R.H.** (2018). Factors influencing heavy metal concentrations in the bottom sediments of the Al-Kharrar Lagoon and Salman Bay, eastern Red Sea coast, Saudi Arabia. *Arabian Journal of Geosciences*, **11**: 495.

Hawes, I., Sumner, D.Y., Andersen, D.T., Jungblut, A.D. and **Mackey, T.J.** (2013) Timescales of growth response of microbial mats to environmental change in an ice-covered Antarctic lake. *Biology, Special Issue on Polar Microbiology,* **2**: 151-176.

Ions, K., Karunarathna, H., Reeve, D.E., Pender, D. (2021). Gravel barrier beach morphodynamic response to extreme conditions. *J. Mar. Sci. Eng*., **9**: 135.

Jorgensen, B.B., Revsbech, N.P. and **Cohen, Y.** (1983). Photosynthesis and structure of benthic microbial mats: microelectrode and SEM studies of four cyanobacterial communities. *Limmology and Oceanography*, **28**: 1075-1093.

Koiwa, N., Takahashi, M., Sugisawa, S., Ito, A., Matsumoto, H., Tanavud, C. and **Goto K.** (2018). Barrier spit recovery following the 2004 Indian Ocean tsunami at Pakarang Cape, southwest Thailand. *Geomorphology,* **306**: 314-324.

Kovalchuk, O., Owttrim, G.W., Konhauser, K.O. and **Gingras, M.K.** (2017) Desiccation cracks in siliciclastic

deposits: microbial matrelated compared to abiotic sedimentary origin. *Sediment Geol*, **347**: 67-78.

Krylenkoa, M.V., Krylenkoa, V.V. and **Volkova, T.A.** (2018). Development prospects of natural-territorial complex of the Dolgaya spit. *Ocean and Coastal Management,* **166**: 98-102.

Maisano, L., Cuadrado, DG. and **Gómez, E.A.** (2019). Processes of MISS-formation in a modern siliciclastic tidal flat, Patagonia (Argentina). *Sedimentary Geology,* **381**: 1–12.

Meshal, A.H. (1987). Hydrography of a Hypersaline Coastal Lagoon in the Red Sea. Estuarine, *Coastal and Shelf Science*, **24**:167-175.

Noffke, N. (2000). Extensive microbial mats and their influences on the erosional and depositional dynamics of a siliciclastic cold water environment (Lower Arenigian, Montagne Noire, France). *Sed. Geol.,* **136**: 207-215.

Noffke, N. (2010) *Microbial Mats in Sandy Deposits from the Archean Era to Today*. Springer- Verlag, Berlin, 194 pp.

Noffke, N., Gerdes, G., Klenke, T. and **Krumbein, W.E.** (2001). Microbially induced sedimentary structures: a new category within the classification of primary sedimentary structures. *J. Sed. Res*., **71**: 649-656.

Noffke, N., Knoll, A.H. and **Grotzinger, J.P.** (2002). Sedimentary controls on the formation and preservation of microbial mats in siliciclastic deposits: a case study from the Upper Neoproterozoic Nama Group, Namibia. *Palaios*, **17**: 533-544.

Noffke, N. and **Paterson, D.** (2008). Microbial interactions with physical sediment dynamics, and their significance for the interpretation of Earth's biological history. *Geobiology*, **6**: 1-4.

Or, D., Smets, B.F., Wraith, J.M., Dechesne, A. and **Friedman, S.P.** (2007). Physical constraints affecting bacterial habitats and activity in unsaturated porous media–a review. Adv. *Water Resour*. **30**: 1505-1527.

Otvos, E.G. (2020)._ Coastal barriers - fresh look at origins, nomenclature and classification issues. *Geomorphology*, **355**: 107000.

Oren, A. (2010) Mats of filamentous and unicellular cyanobacteria in hypersaline environments, in Microbial Mats. *Cellular Origin, Life in Extreme Habitats and Astrobiology*, **14**: 387-400.

Pan, J., Cuadradodg and **Bournod, C.N.** (2017). Diatom-driven recolonization of microbial mat-dominated siliciclastic tidal flat sediments. *FEMS Microbiology Ecology*, **93**, 2017, fx111. doi: 10.1093/femsec/fx111

Pan, J., Perillo, V.L. and **Cuadrado, D.G.** (2019). Quantifcation of microbial mat response to physical disruption in siliciclastic sediments. *Estuarine, Coastal and Shelf Science*, **230**: 106434.

Paterson, D. (1994) Microbial mediation of sediment structure and behaviour. In: Microbial Mats (Eds Stal, L. and Caumette, P.), *Ecological Studies*, **35**: 97–109. Springer, Berlin, Heidelberg, New York.

PME (Presidency of Meteorology and Environment) (2015) *Data of the climatic elements of Jeddah through 1980–2015. Kingdom of Saudi Arabia, Jeddah*

Porada, H., Bouougri, E.H. and **Ghergut, J.** (2007). Hydraulic conditions and mat-related structures in tidal flats and coastal sabkhas. In: Schieber, J., Bose, P.K., Eriksson, P.G., Banerjee, S., Altermann, W., Catuneanu, O. (Eds.), *Atlas of Microbial Mat Features Preserved Within the Clastic Rock Record*. Elsevier, pp. 258–265

Rabaa, S.M.A. (1980). Geomorphological characteristics of the Red Sea coast with special emphasis on the formation of Marsas in the Sudan. *Proceedings of a Symposium on Coastal and Marine Environments of the Red Sea, Khartum, 2. Alesco/RSC, University of Khartum*.

Rasul, N.M.A. (2015). Lagoon sediments of the eastern Red Sea: distribution processes, pathways and patterns. In: Rasul, N.M.A. and Stewart I.C.F. (eds.), *The Red Sea*, Springer Earth System Sciences, pp. 281-316.

Reineck, H.-E., Gerdes, G., Claes, M., Dunajtschik, K., Riege, H. and **Krumbein, W.E.** (1990). Microbial modification of sedimentary surface structures. In: D. Heling: Rothe, U. Förstner and P. Stoffers (Eds), *Sediments and Environmental Geochemistry*. Selected aspects and case histories, pp. 254-276. Springer; Berlin.

Sander, L., Michaelis, R., Papenmeier, S., Pravkin, S., Mollenhauer, H., Grotheer, H., Gentz, T. and **Wiltshire, K.H.** (2019). Indication of Holocene sea-level stability in the southern Laptev Sea recorded by beach ridges in north-east Siberia, Russia. *Polar Res*. **38**: 3379.

Schieber, J. (1999). Microbial mats in terrigenous clastics: the challenge of identification in the rock record. *PALAIOS* **14**: 3-12.

Schieber, J. (2004). Microbial mats in the siliciclastic rock record: a summary of diagnostic features. In: Eriksson, P.G., Altermann, W., Nelson, D., Mueller, W.U., Catuneanu, O., Strand, K. (Eds.), *The Precambrian Earth: Tempos and Events, Developments in Precambrian Geology*. Elsevier, pp. 663–672

Shepard, R.N. and **Sumner, D.Y.** (2010). Undirected motility of filamentous cyanobacteria produces reticulate mats. *Geobiology*, **8**: 179–190.

Staats, N., Stal, L.J., de Winder, B. and **Mur, L.R.** (2000). Oxygenic photosynthesis as driving process in exopolysaccharide production of benthic diatoms. *Mar. Ecol. Prog. Ser.*, **193**: 261–269.

Stal, L. J. (2010). Microphytobenthos as a biogeomorphological force in intertidal sediment stabilization. *Ecological Engineering*, **36**: 236–245.

Stal, L. J. (2012). Cyanobacterial mats and stromatolites. In: Whitton, B.A. (Eds.), *Ecology of Cyanobacteria II: Their Diversity in Space and Time*. Springer, Dordrecht, pp. 65-125

Stéphan, P., Suanez, S. and **Fichaut, B.** (2015). Long-, mid- and short-term evolution of coastal gravel spits of Brittany, France. In: G. Randazzo; D. Jackson; A. Cooper (Eds.), *Sand and Gravel Spits*, 12, Coastal Research Library, Springer, pp.275-288.

Stolz, J.F. (2000). *Structure of microbial mats and biofilms. Microbial Sediments*. Springer, pp. 1-8.

Sumner, D.Y., Jungblut, A.D., Hawes, I., Andersen, D.T., Mackey, T.J. and **Wall, K.** (2016) Growth of elaborate microbial pinnacles in Lake Vanda, *Antarctica. Geobiology*, **14**: 556-574.

Taj, R., Aref, M. A. and **Schreiber, B. C.** (2014). The influence of microbial mats on the formation of sand volcanoes and mounds in the Red Sea coastal plain, south Jeddah, Saudi Arabia. *Sedimentary Geology*, **311**: 60-74.

Youssef, M. (2015) Heavy metals contamination and distribution of benthic foraminifera from the Red Sea coastal area, Jeddah, Saudi Arabia. *Oceanologia*, **57**: 236-250.

التراكيب الأولية الرسوبية الميكروبية ودورها في تثبيت الرواسب وتكوين التضاريس الحصوية الساحلية (الحيود والألسنة والحواجز) في بحيرة سلمان شديدة الملوحة، ساحل البحر الأحمر بالمملكة العربية السعودية

عمار عبدالجليل مناع

قسم الجيولوجيا البحرية، كلية علوم البحار، جامعة الملك عبد العزيز، جدة، المملكة العربية السعودية

المستخلص. تشير هذه الدراسة إلى تواجد أشكال عديدة من التراكيب الأولية الرسوبية الميكروبية، مثل: الصفائح الميكروبية الرقيقة، وعلامات النيم المثبتة حيويا، والقباب الغازية، والطيات الميكروبية، وجيوب وبقايا التعرية، والشقوق الميكروبية، وشرائح ميكروبية جبسية في بحيرة سلمان شديدة الملوحة، شمال مدينة جدة، المملكة العربية السعودية. وتذكر هذه الدراسة أن العمليات الميكروبية والفيزيائية تؤدي إلى الثبات الحيوي للرواسب وتكوين الألسنة والحواجز والحيود الساحلية. وتركز هذه الدراسة على دور الأمواج المتكونة بنشاط الرياح في تعرية الرواسب المثبتة حيويًا بالصفائح الميكروبية، وترسيبها على الشاطئ الشرقي لبحيرة سلمان شبه المغلقة. في شهور الشتاء، تتكون علامات النيم على أرضية البحيرة، والتي يغطيها صفائح ميكروبية خضراء وسوداء. أما في شهور الصيف، فتنمو بلورات الجبس على سطح الصفائح الميكروبية، وتكون قشرة جبسية ميكروبية. ويحدث في شهور الشتاء، أن الحركة الطفيفة لمياه البحيرة تؤدي إلى تعرية الصفائح الميكروبية، والتي تسبب اللون الأسود لمياة البحيرة. أما في شهور الصيف، فإن الحركة القوية للأمواج المتكونة بنشاط الرياح القوية تؤدي إلى تعرية القشرة الجبسية الميكروبية والطبقات السفلية للرواسب الحيوية والجبسية، وتكون شرائح ميكروبية حصوية، والتي تترك جيوبًا ومنخفضات التعرية المحاطة ببقايا مرتفعة من الصفائح الميكروبية. وتنتقل رواسب التعرية الحصوية عن طريق التيارات الساحلية الطويلة، ثم تترسب على الشاطئ الشرقي للبحيرة على هيئة حيود وألسنة وحواجز ساحلية. ويتكون خلف هذه الألسنة والحواجز الساحلية برك ضحلة مغطاه برواسب الغرين. تقدم نتائج هذه الدراسة بيانات مفيدة للتنبوء بالعمليات المسببة لتغيرات التضاريس الساحلية نتيجة تثبيت الرواسب حيويًا عن طريق الصفائح الميكروبية، ثم تعريتها بالأمواج المتكونة بالرياح.